

INTRODUCTION TO LM26

Lawson Machine 26 (LM26) is a magnetized target fusion (MTF) demonstration machine with the goal of producing significant plasma heating via compression.

Operation

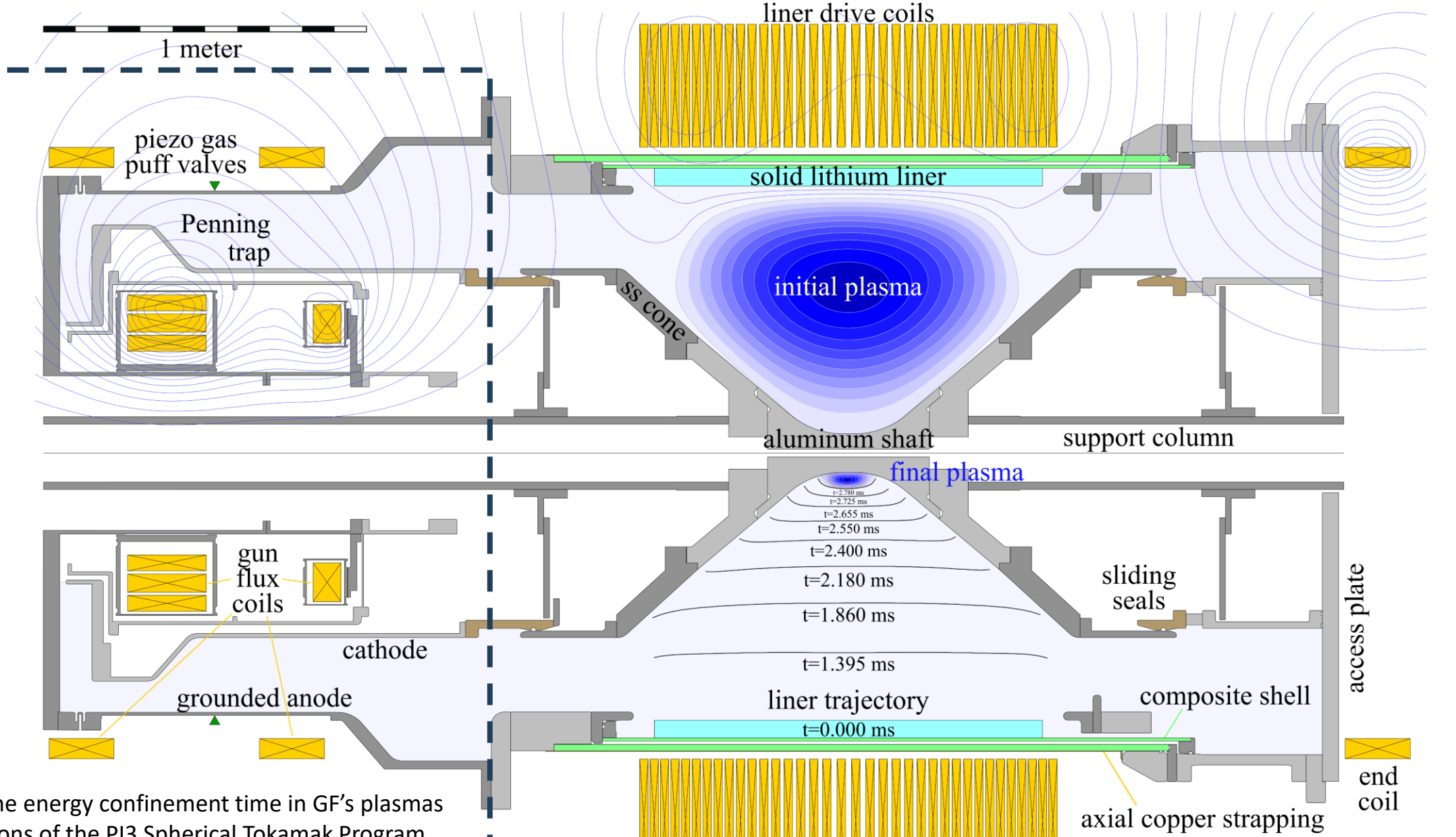
- 1. The toroidal plasma is generated by coaxial helicity injection (CHI).
2. Plasma confined inside a solid lithium liner, with an aluminum shaft.
3. Liner inductively compressed in less than 3 milliseconds.
4. The plasma will heat if the energy confinement time is longer than the compression time.
5. Plasma must remain MHD stable throughout the whole compression to maintain confinement.

Status

- Design of the first stage is complete.
• Simulations of the machine operation and performance are mature.
• Construction of the 18 MJ power supply is underway
• Large components of the flux conserver are being manufactured.
• PI3 CHI injector is being disassembled to be reconfigured as LM26.
• First plasma is scheduled for Q1 2025.
• Goal is to reach 10 keV by 2025.

Plasma Compression Experiment Design

QR code for video of LM26 Concept www.youtube.com/watch?v=3i3hPtWQ0LU



Plasma Injector 3 (PI3)

- Largest coaxial helicity injector ever built.
• In operation since 2018 with an almost spherical aluminum flux conserver.

Table with 4 columns: Parameter, Value 1, Value 2, Unit. Rows include Poloidal flux, Plasma current, Shaft current, Plasma density, Temperature, and Confinement time.

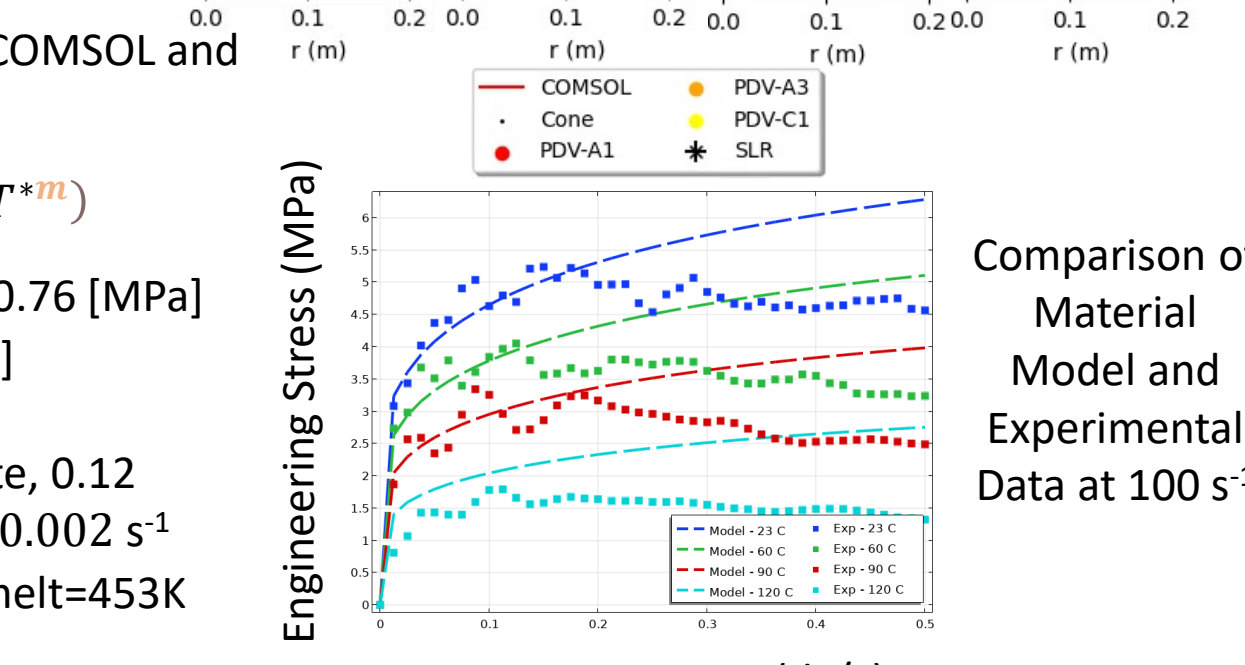
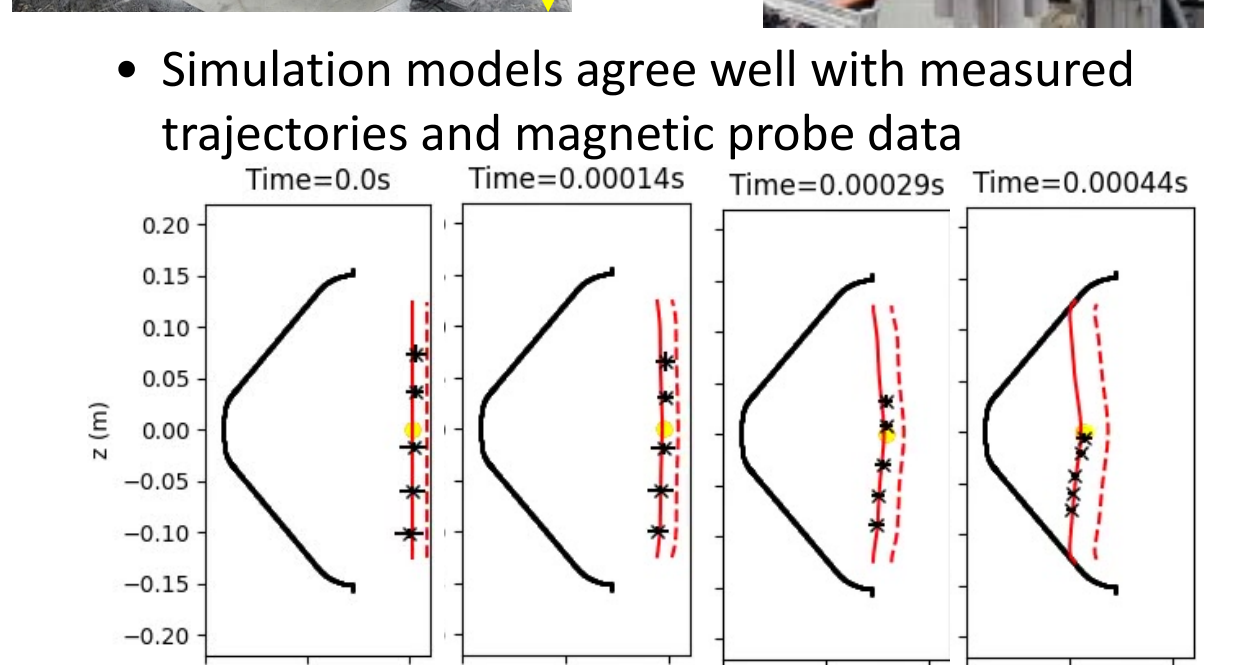
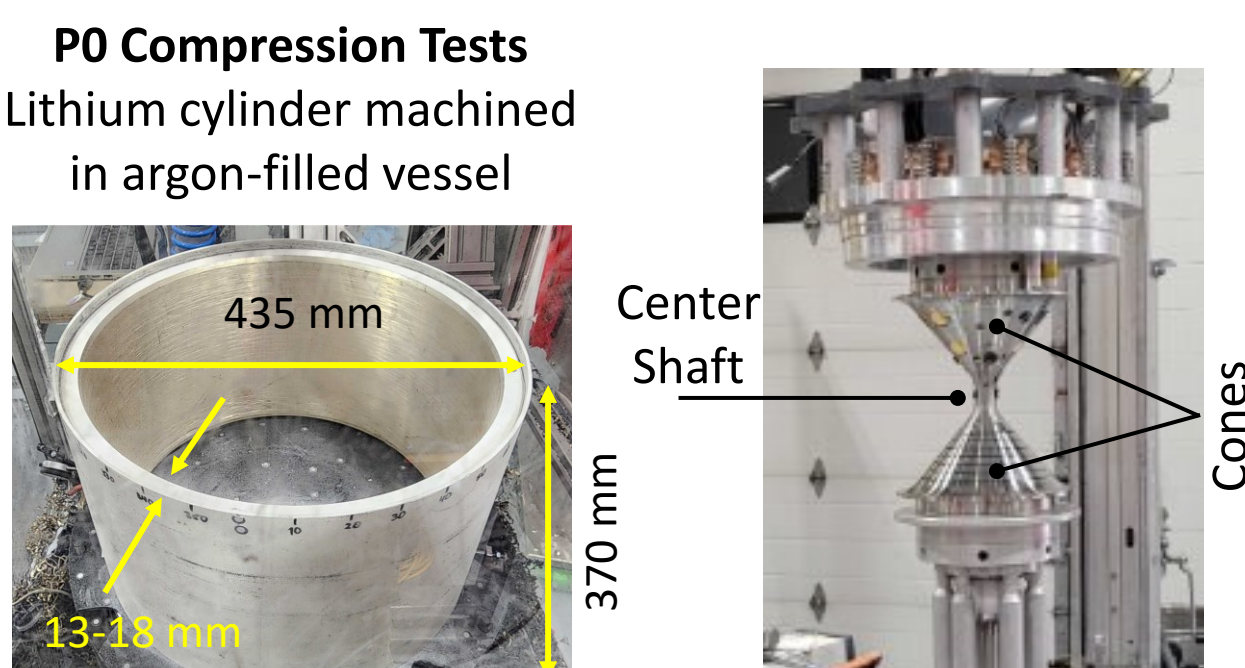
Related talks and posters:
GO05.00012: Andrea Tancetti (Tues 11:42-11:54 AM) Calculation of the energy confinement time in GF's plasmas
JP12.00111: Patrick Carle (Tues 2:00-5:00 PM) Physics Conclusions of the PI3 Spherical Tokamak Program

Table comparing LM26 Plasma Geometry parameters (Initial Value and Final Value) with capacitor bank specifications (Voltage, Capacitance, Energy).

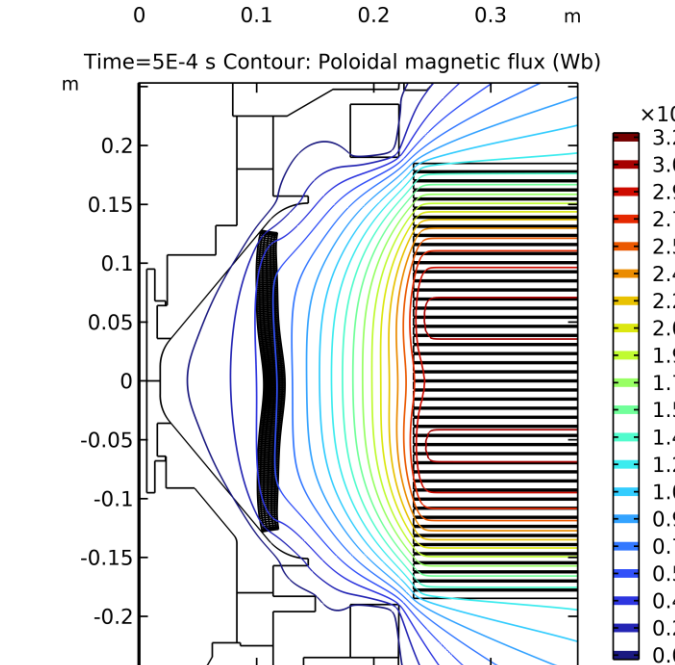
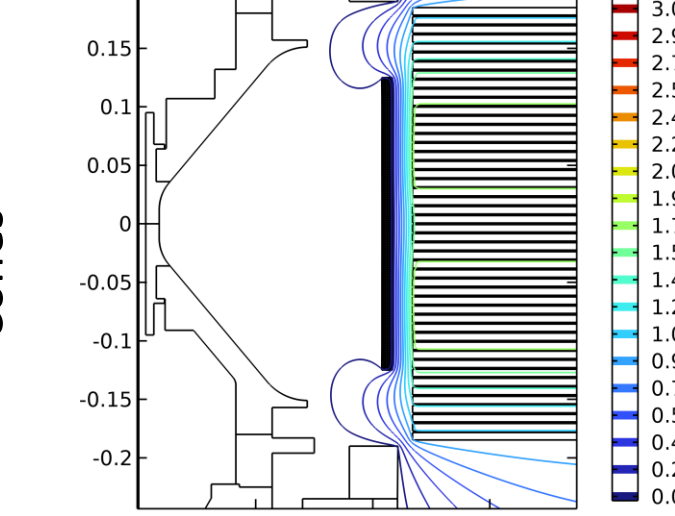
COMSOL MODEL VALIDATION WITH EXPERIMENT

Steps for Model Implementation

- 1. Lithium material characterization
2. Validate with lithium ring compression experiments
3. Validate lithium cylinder compression on cones
4. Trajectory prediction in full-scale LM26 geometry



Simulation of Prototype Zero (P0), liner acceleration experiment



Max compression is reached at 0.8 ms. Cavity radius has been reduced by a factor of about 5.

Johnson-Cook Material Model, calibrated with COMSOL and PolymerFEM Mcalibration.
Equation: sigma_y = (sigma_y + B*epsilon_p^n) * (1 + C*ln(epsilon/epsilon_ref)) * (1 - T**m)

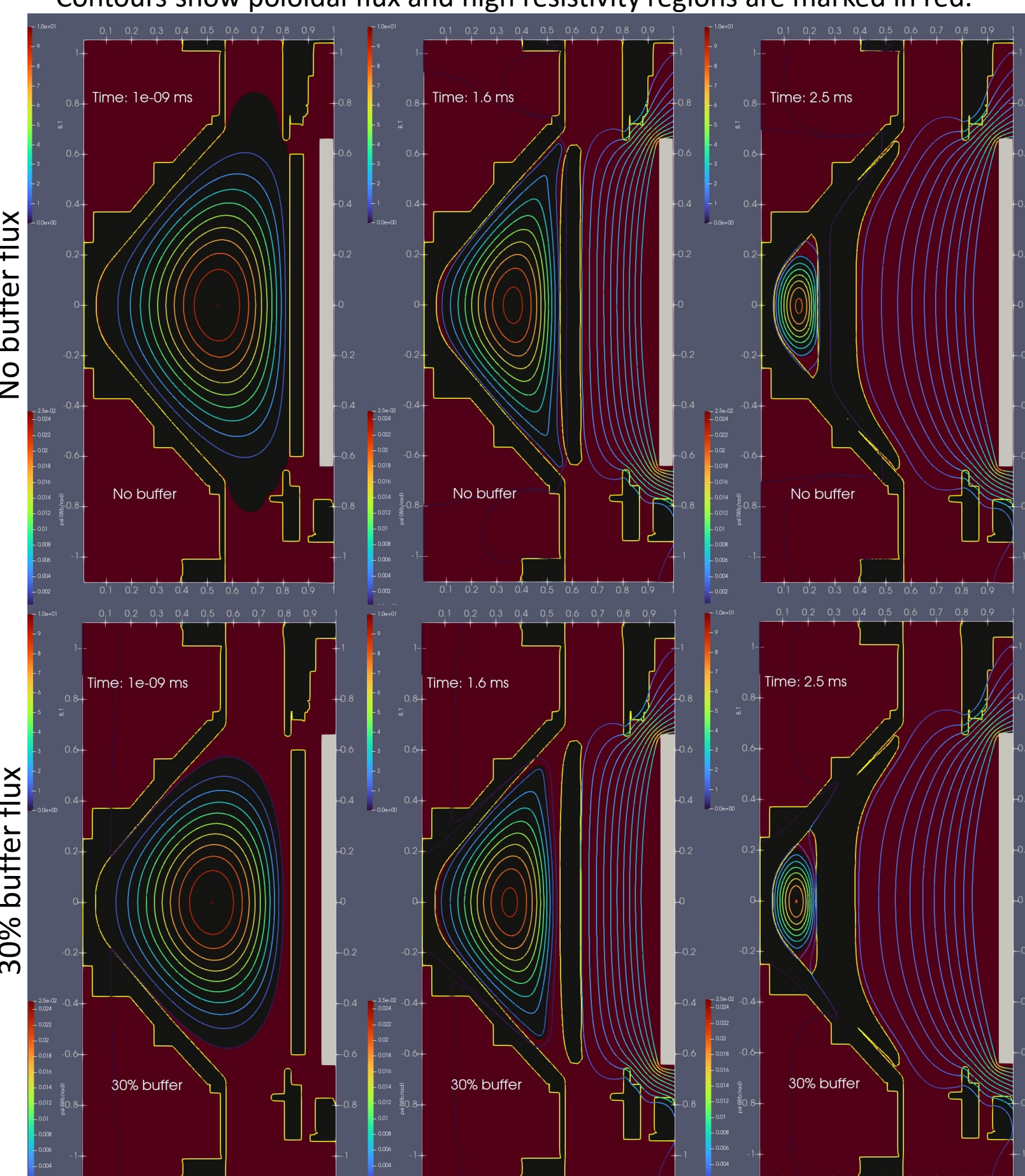
- sigma_y: Yield stress at reference conditions, 0.76 [MPa]
• B: Strain hardening constant, 2.96 [MPa]
• n: Strain hardening coefficient, 0.31
• C: Strengthening coefficient of strain rate, 0.12
• epsilon_p: Plastic strain, reference rate epsilon_ref = 0.002 s^-1
• T*: temperature (T-294)/(Tmelt-294), Tmelt=453K
• m: Thermal softening coefficient, 1.27

OPENFOAM MHD MODEL VALIDATION

The OpenFOAM MHD solver developed at General Fusion [V Suponitsky et al. Fluids 2022, 7(7), 210] was extended to simulate EM compression of the liner driven by the external circuit and diffusion of the magnetic fields into multiple solid materials.

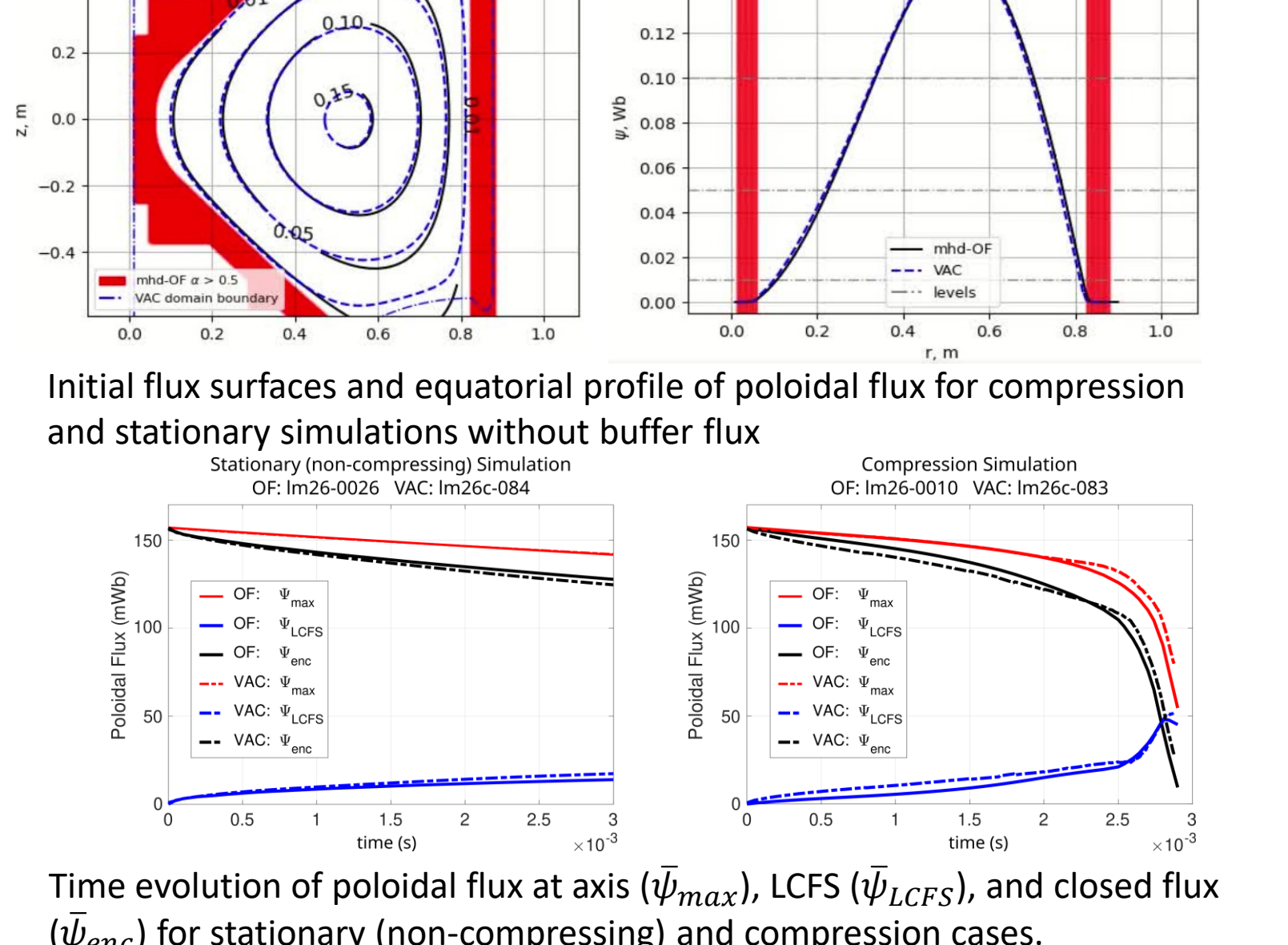
The solver is used to simulate: (1) small ring compressor, (2) P0 experiments with emphasis on toroidal flux trapping and flux diffusion into the cones, and (3) compression of a simplified magnetized plasma in LM26, which involves interaction between plasma magnetic fields, buffer fields, and driving fields.

LM26 plasma compression simulations with 0% and 30% buffer flux



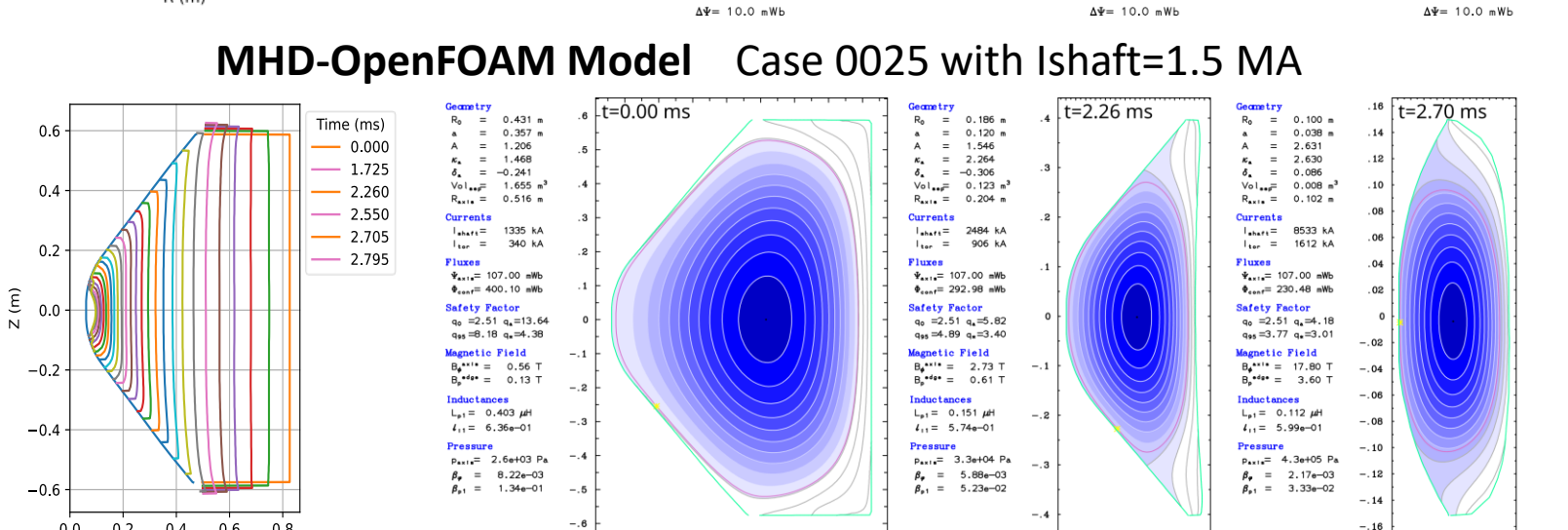
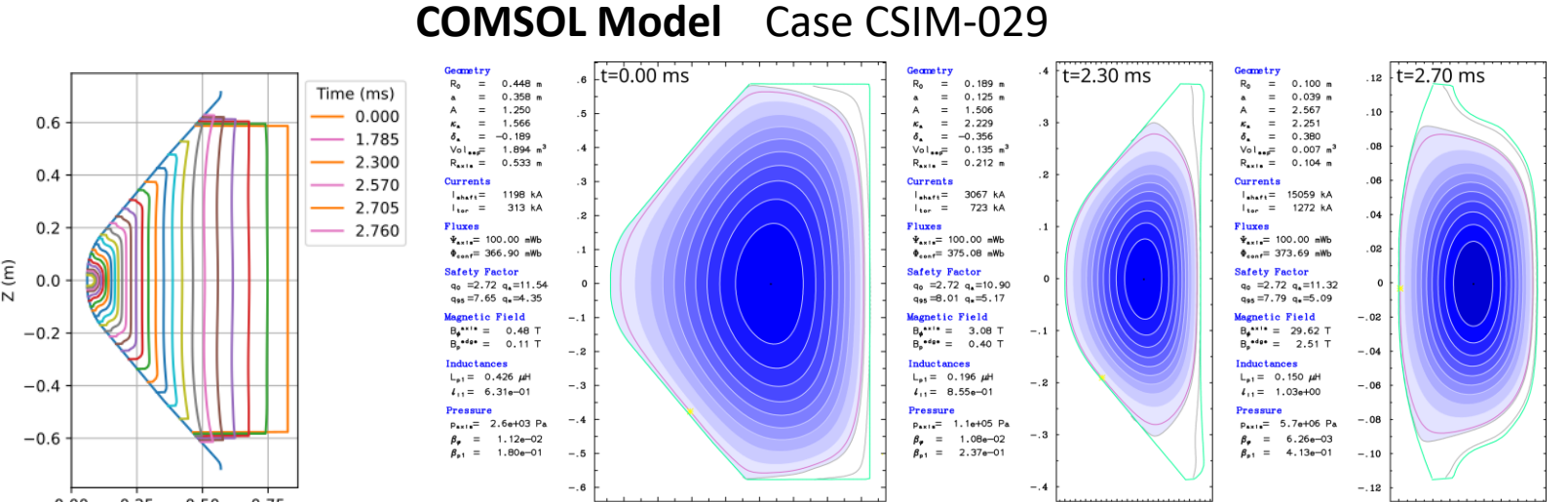
• Plasma region bounded by LCFS, with high resistivity (red) outside
• Buffer field controls shape of the plasma and diffusion into liner and cones
• With buffer flux plasma is limited on the cones. Choice of materials plays an important role in reducing flux diffusion.

Comparison between MHD-OpenFOAM solver and layered VAC



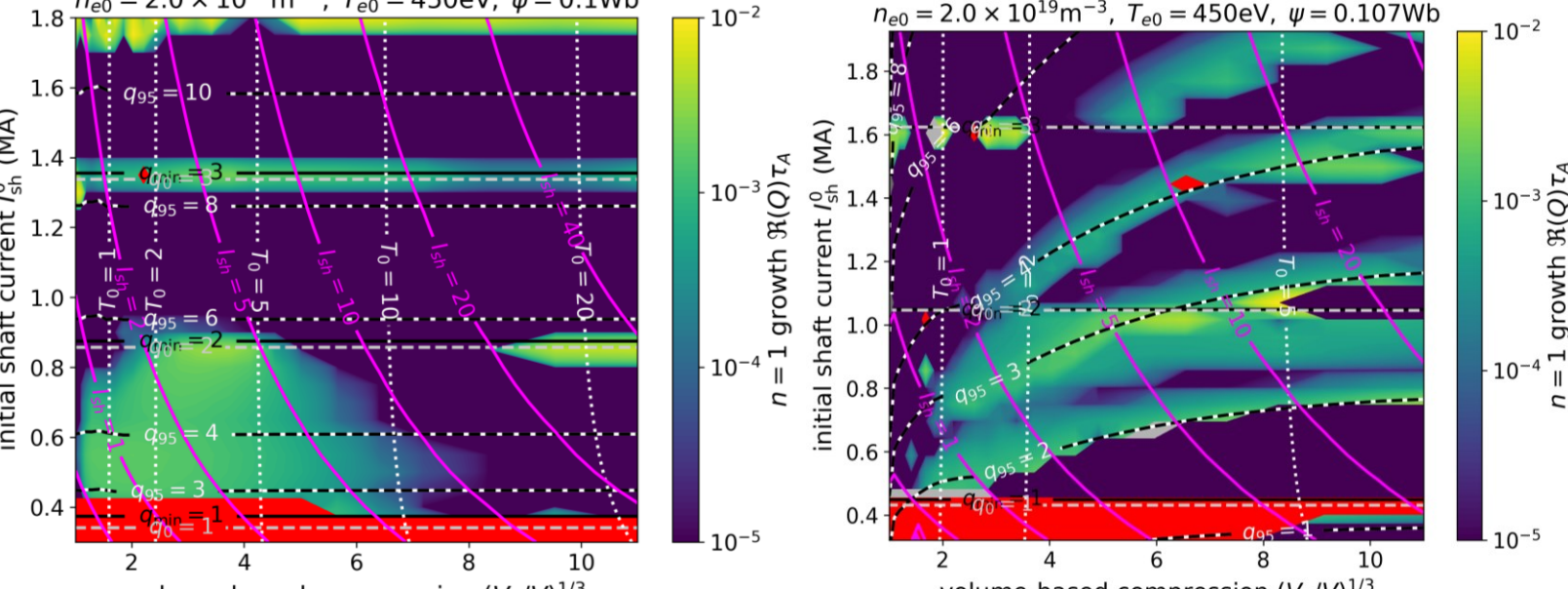
MHD STABILITY DURING COMPRESSION

The plasma will heat to fusion conditions only if compressional heating is greater than transport losses, i.e., if the energy confinement time is longer than the compression time. To maintain sufficient energy confinement time, the plasma must be kept MHD stable.



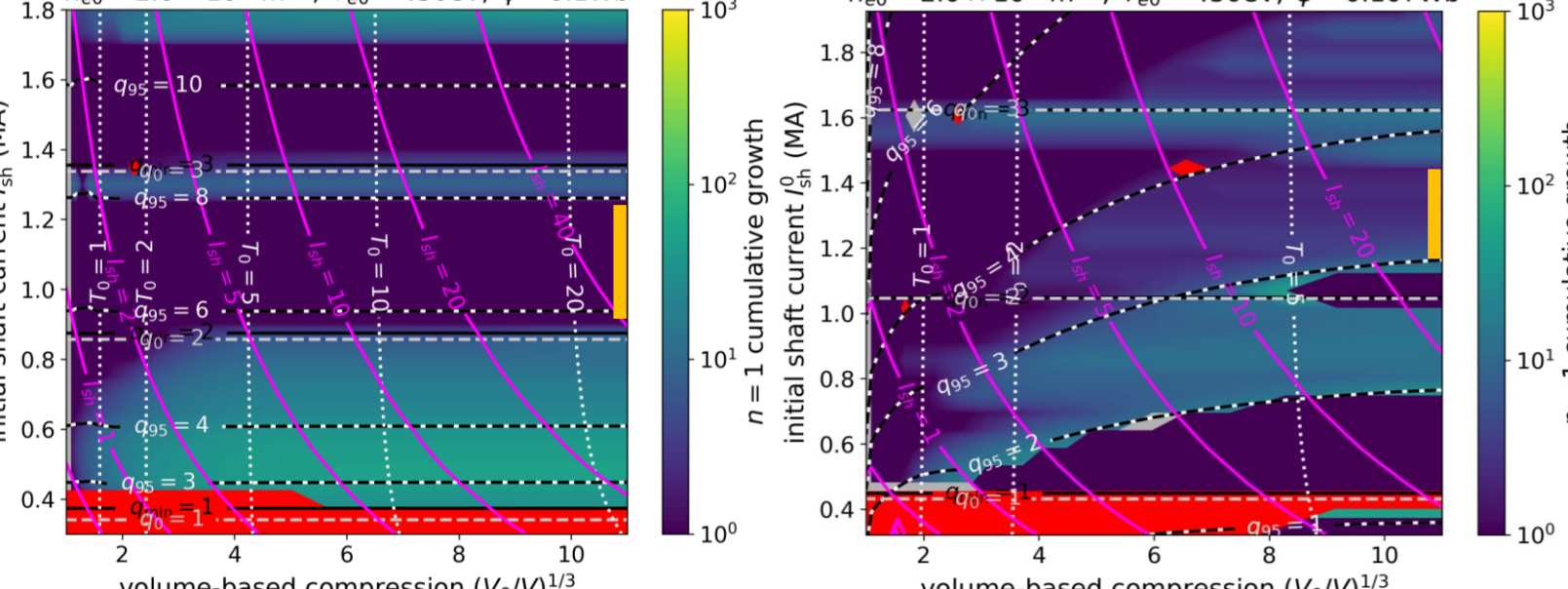
• We introduce the same plasma in both trajectories, with only the geometry and poloidal flux boundary conditions taken from COMSOL and OpenFOAM.
• Case CSIM-029 has small (~4 mWb) flux diffusion through liner from drive coils.
• Case OFSIM-0025 uses an isothermal MHD plasma and models flux diffusion from the plasma into the flux conserver.
• Despite these differences, the liner trajectories and poloidal flux boundary conditions are very similar until late compression (>V/V_0 = 5^3).

Stability Map for COMSOL geometry Stability Map for OpenFOAM geometry



• Horizontal trajectories show properties of plasmas that have conserved safety factor (q) and specific entropy profiles
• Red regions = ideal MHD unstable (very fast growth)
• Yellow/Green regions = resistively unstable (fast/slow)
• Deep blue regions = stable
• Magenta = shaft currents (I_shaft) given in MA

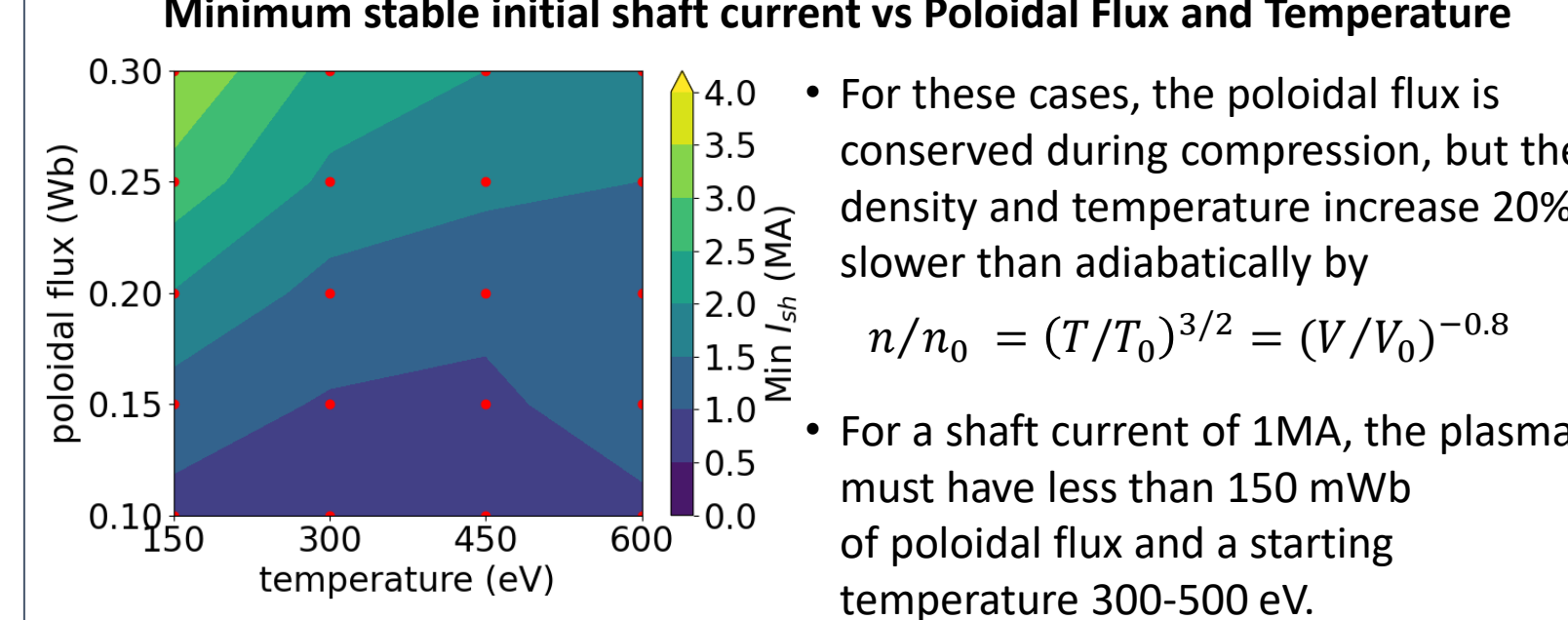
Perturbation Growth for COMSOL Perturbation Growth for OpenFOAM



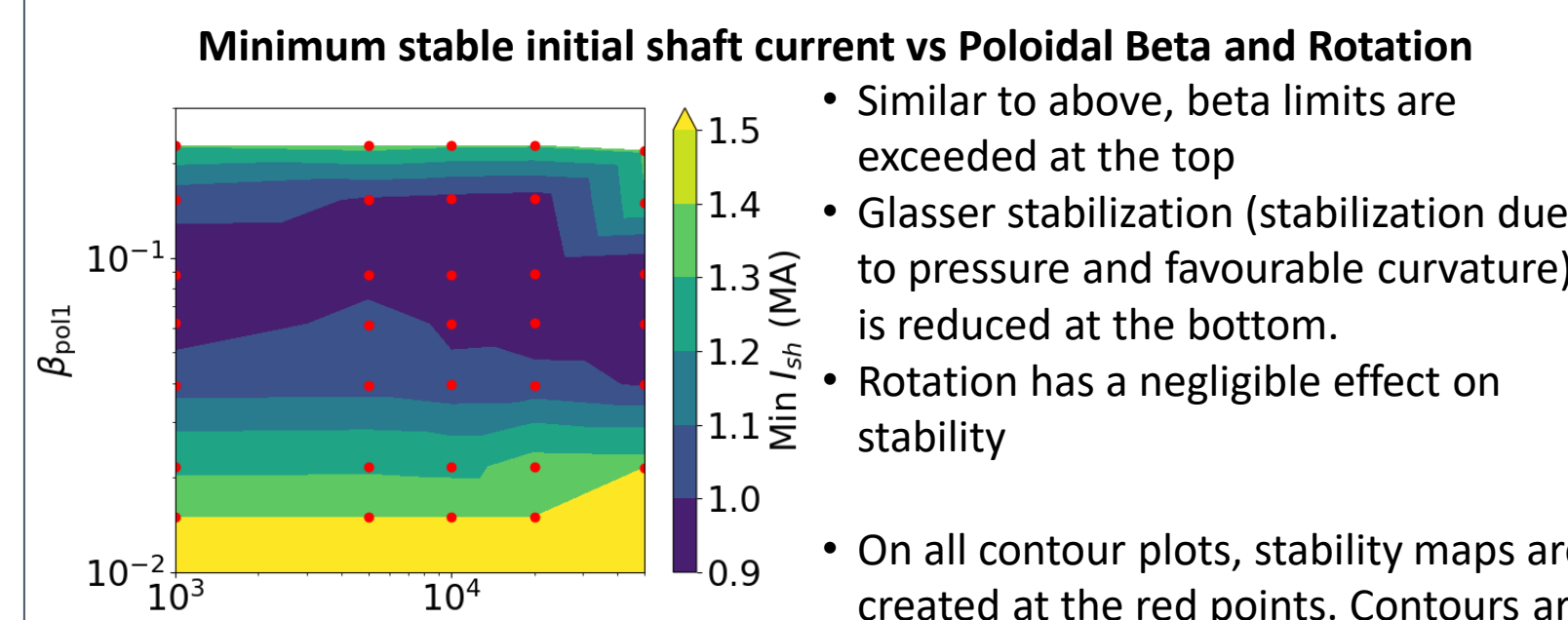
• We assume that the plasma can tolerate perturbation growth of 10 times before final compression and use that as a threshold to find stable corridors.
• Under this criterion, both COMSOL and OpenFOAM trajectories agree that plasmas remain stable until full compression when q_min = 2.3-2.7 (orange line).
• Flux and q conservation cause a peaked edge current as geometry changes.
• Edge q decreases in OpenFOAM model because flux surfaces diffuse into shaft.

REQUIREMENTS FOR PLASMA STABILITY

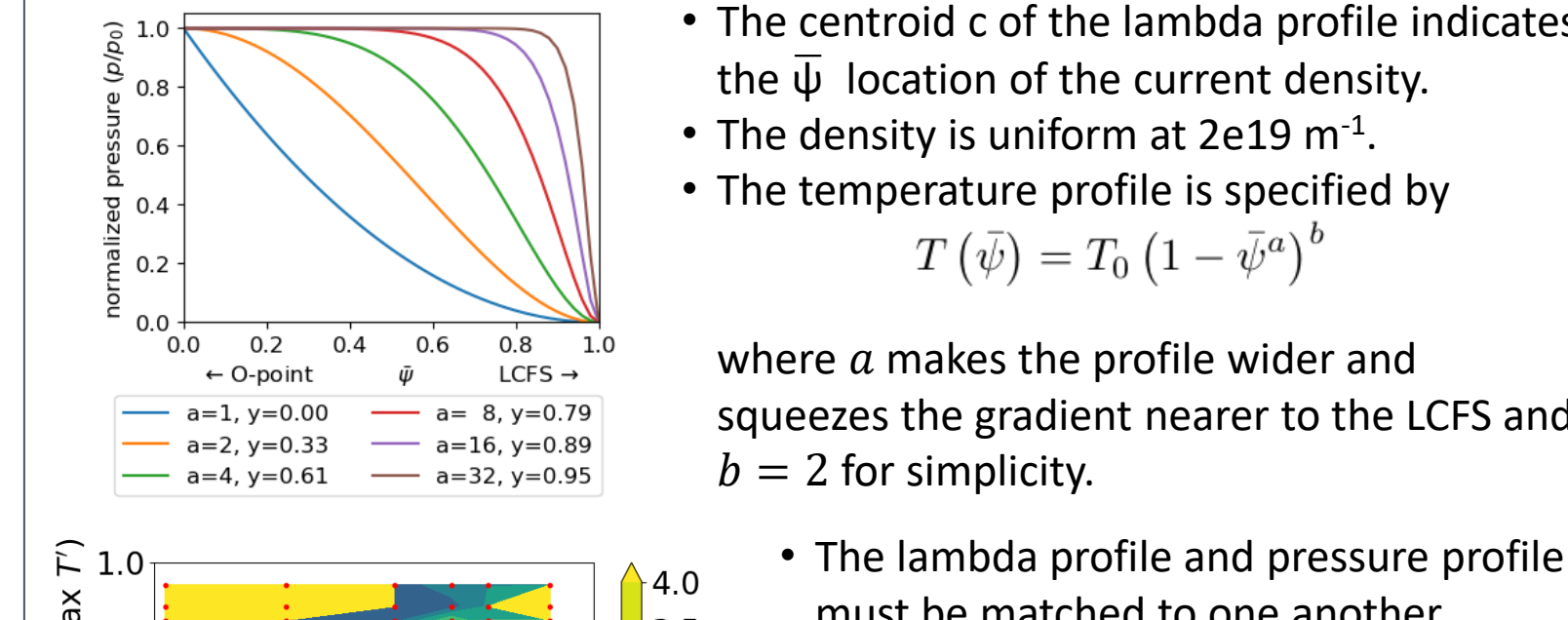
MHD stability can usually be achieved by increasing shaft current and, hence, the toroidal field and safety factor q. However, generating shaft current requires large, expensive capacitors. We want to know the minimum necessary shaft current that will maintain stability through to the end of the compression trajectory.



• For these cases, the poloidal flux is conserved during compression, but the density and temperature increase 20% slower than adiabatically by n/n_0 = (T/T_0)^{3/2} = (V/V_0)^{-0.8}
• For a shaft current of 1MA, the plasma must have less than 150 mWb of poloidal flux and a starting temperature 300-500 eV.



• Beta limits are exceeded in top right
• Glasser stabilization (stabilization due to pressure and favourable curvature) is reduced in bottom left.
• Resistivity is less on the right, so bottom right is most stable and less shaft current is required there.
• In yellow regions, the shaft current required to achieve stability exceeds the maximum viable stability.

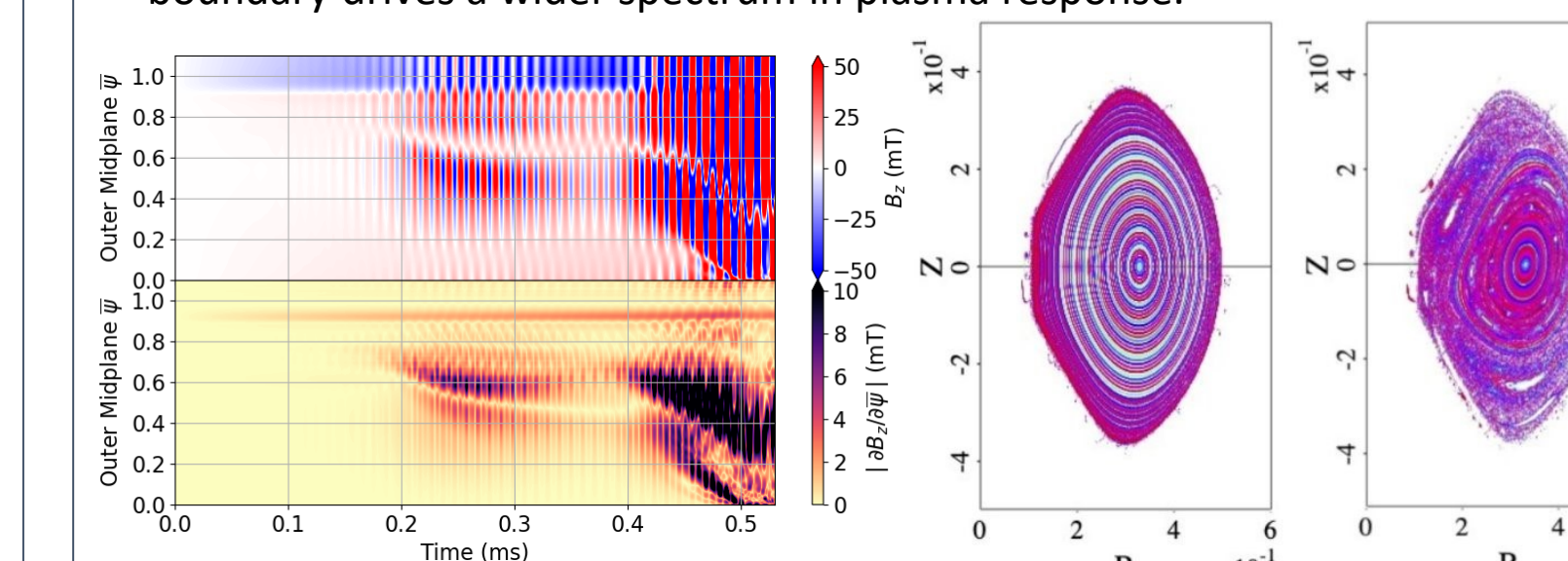


• Similar to above, beta limits are exceeded at the top
• Glasser stabilization (stabilization due to pressure and favourable curvature) is reduced at the bottom.
• Rotation has a negligible effect on stability
• On all contour plots, stability maps are created at the red points. Contours are interpolated from those points.

ERROR FIELD PENETRATION

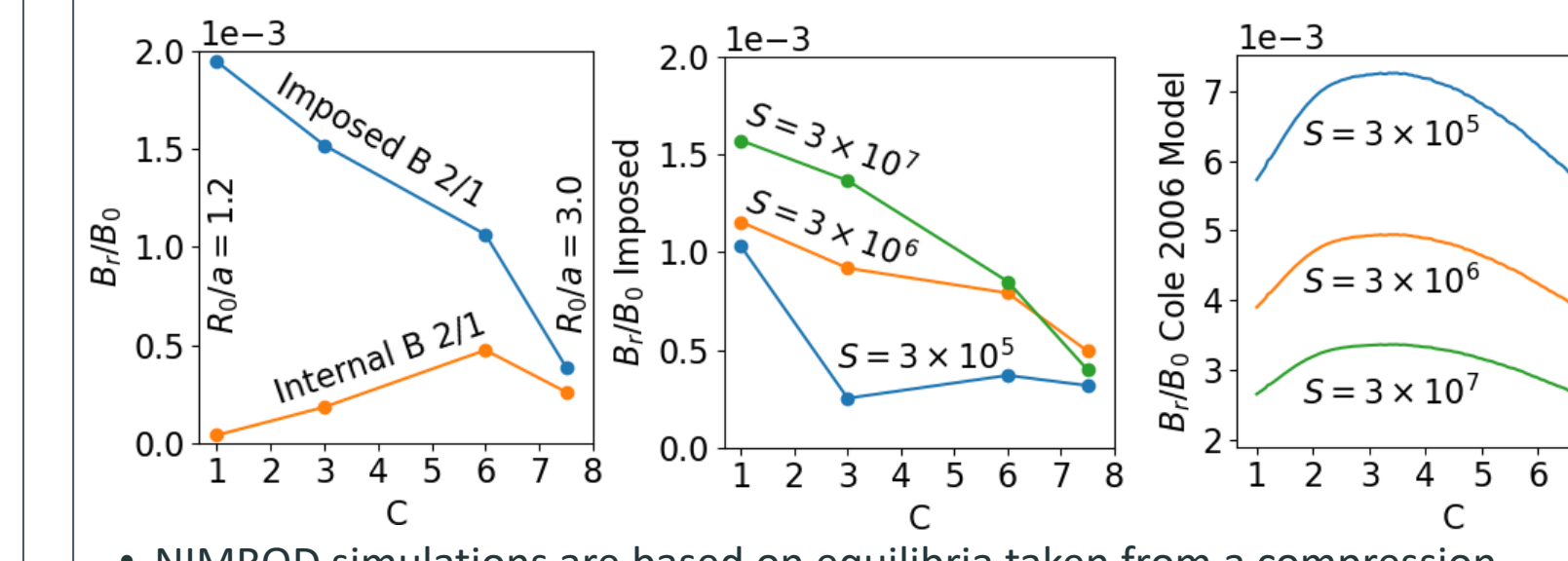
Geometric perturbations in the liner surface will grow during compression and be experienced by the plasma as increasing magnetic perturbations, or error fields. Error field penetration (EFP) is an important problem in the stable regions and can drive resonant perturbations in the plasma.

- We take a two-pronged approach:
o Reduced model of Cole and Fitzpatrick [A Cole, R Fitzpatrick 2006 Phys. Plasmas 13 032503] applied to equilibria
o NIMROD simulations with RMP boundary imposed
• The goal is to characterize the penetration thresholds and find the conditions (e.g. resistivity, viscosity, rotation, etc.) that shield the highest error fields.
• We analyze in a static equilibrium geometry, which is justified because the compression time is much longer than Alfvén time and RMP ramp time.
• Resonant magnetic perturbation (RMP) of 2/1 mode imposed on Br at boundary drives a wider spectrum in plasma response.

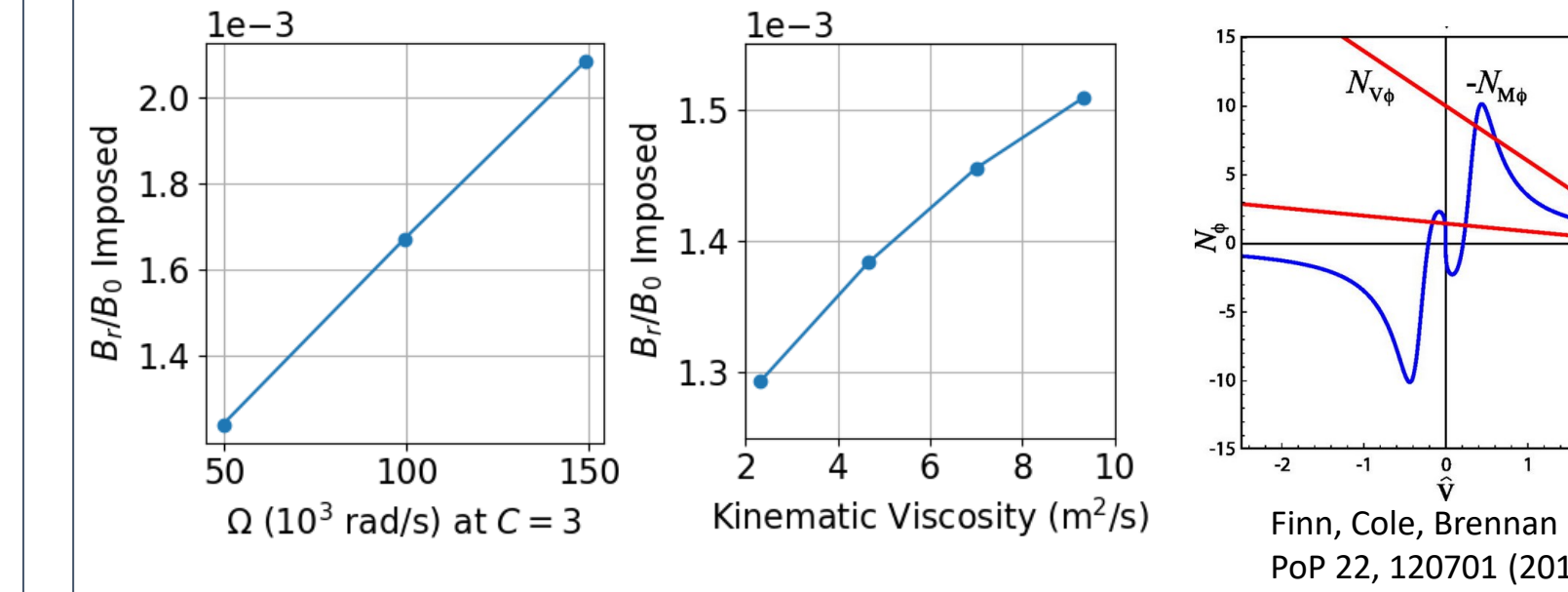


Bz on outer midplane of NIMROD plasma showing penetration at 0.2 ms.

• Prior to penetration, initial islands can propagate, as described by Fitzpatrick model [PoP 21, 092513 (2014)] and observed by Howell [NIMROD Mtg 5/23].
• Penetration point is deduced where the island width rapidly grows past the layer width, such as at t=0.2 ms in Br phase plot above.



• NIMROD simulations are based on equilibria taken from a compression sequence. In addition to constraints on entropy and q, the toroidal flow omega increases by angular momentum conservation.
• Aspect ratio, shaping, and Omega affect the plasma response spectrum (ratio of 2/1 inside), but fixing Lundquist number (S) isolates those effects.
• EFP limits from NIMROD start at (10^-3) and decrease with modestly with C and S, unlike analytic model [Cole & Fitzpatrick, Phys. Plas. 13, 032503 (2006)] where high S cases have lower limits and effect of C is non-monotonic.



• NIMROD results at lower Lundquist number S = 5 x 10^5 are not fully in the asymptotic regime and deviate significantly from analytic model.
• Increases in S and Omega are most impactful on penetration thresholds.

Future Error Field Penetration Work

- Understand discrepancies between NIMROD and Cole 2006 analytic model.
• Penetration limits ~1e-3 pre-compression decrease to ~1e-4 as S increases.
o How important are experimentally observed rotation shears?
o How important is the shaping and stability to the EFP limits?
o Are two fluid effects important?
• Kinetic ions interactions and kinetic layer regimes all open questions
• Flux soak into wall affects the equilibrium and EFP limits and will be included
• Instability interaction with the liquid wall also being investigated